

Radioastron (Spectr-R Project)—A Radio Telescope Much Larger than the Earth: Ground Segment and Key Science Areas

Yu. A. Alexandrov^a, V. V. Andreyanov^a, N. G. Babakin^a, V. E. Babushkin^b, K. G. Belousov^a,
A. A. Belyaev^c, A. V. Biryukov^a, A. E. Bubnov^a, A. A. Bykadorov, V. I. Vasil'kov^a, I. S. Vinogradov^a,
A. S. Gvamichava^a, A. N. Zinoviev^a, R. V. Komaev^b, B. Z. Kanevskiy^a, N. S. Kardashev^a,
Yu. A. Kovalev^a, Yu. Yu. Kovalev^a, A. V. Kovalenko^a, Yu. A. Korneev^a, V. I. Kostenko^a, B. B. Kreisman^a,
A. Yu. Kukushkin^a, M. G. Larionov^a, S. F. Likhachev^a, L. N. Likhacheva^a, S. Yu. Medvedev^c,
M. V. Melekhin^b, T. A. Mizyakina^a, N. Ya. Nikolaev^a, B. S. Novikov^a, I. D. Novikov^a, Yu. K. Pavlenko^c,
Yu. N. Ponomarev^a, M. V. Popov^a, V. N. Pyshnov^a, V. M. Rozhkov^e, B. A. Sakharov^c,
V. A. Serebrennikov^b, A. I. Smirnov^a, V. A. Stepanyants^d, S. D. Fedorchuk^a, M. V. Shatskaya^a,
A. I. Sheikhet^b, A. E. Shirshakov^b, and V. E. Yakimov^a

^a Astro Space Center of the Lebedev Physics Institute, Russian Academy of Sciences, Leninskii pr. 53, Moscow, 119991 Russia

^b NPO Lavochkin, Federal Unitary Enterprise, ul. Leningradskaya 24, Khimki, 141400 Russia

^c ZAO Vremya-Ch, Nizhni Novgorod, Russia

^d OAO Russian Space Systems, Russia, Moscow

^e Keldysh Institute of Applied Mathematics, Russian Academy of Sciences, Miusskaya pl. 4, Moscow, 125047 Russia

Abstract—The space interferometer *Radioastron* is working jointly with the largest radio telescopes of the world. Ground tracking stations provide for retrieving the information and determining the orbital parameters for data processing centers. The project is aimed at systematic studies of images of radio emitting regions, their coordinates, and time-dependent variations near super-massive black holes in galactic nuclei, stellar-mass black holes, neutron and quark stars, regions of star and planet formation in our and other galaxies, the structure of interplanetary and interstellar plasma, and the Earth's gravitational field.

Keywords: space interferometer, image synthesis, flow, intensity, polarization, data processing and correlation center

DOI: 10.1134/S0038094612070039

INTRODUCTION

The launch of the space radio telescope (SRT) provides an opportunity to start studying astronomical objects with an angular resolution better by a factor of 30 than the resolution achieved to date. Combined with ground-based radio telescopes, the SRT forms an Earth–space interferometer that has a baseline of up to 350 000 km. Table 1 contains the list of all the large radio telescopes with an effective antenna diameter greater than 60 m; the SRT frequency bands are given for which joint interferometric observations are possible. More detailed data are available at the website [1].

HIGH-INFORMATION SRT RADIO LINK

A high-information radio link was developed and produced in the process of the *Radioastron* project implementation. Via this link, scientific data are transmitted from the spacecraft (SC) to the ground-based receiving complex for subsequent processing, and the service information on the SC and SRT conditions is provided for investigators.

The high-information radio link includes the onboard high-information radio complex (HIRC) (Fig. 1) and the ground-based tracking station based on the RT-22 radio telescope at the Pushchino observatory of the Astro Space Center of the Lebedev Physics Institute (Fig. 2).

The HIRC includes the following components:

(1) A 15-GHz transmitter to transfer scientific and service data obtained during observations. The transmitter power is 40 W; for data modulation, double differential phase shift keying (DDPSK) is used.

(2) A 8.4-GHz transmitter with an output power of 2 W.

(3) A highly sensitive signal receiver at a frequency of 7.2 GHz (the noise temperature is 70 K);

(4) The feed system of the high-gain antenna with a diameter of 1.5 m and a tracking drive for accurate pointing to ground-based tracking stations (GTSs).

A ground tracking station (GTS) is designed for the following tasks:

(1) Pointing the GTS antenna and tracking the spacecraft during the communication session.

(2) Receiving the flow of scientific and service data from the SC; recording the data on hard drives.

(3) Transmitting a phase-stable reference signal synchronized by an H-maser of the GTS to the SC.

(4) Receiving the response signal that was coherently transformed on board the SC, measuring the current frequency of a residual Doppler shift and current phase difference between the response and request signals, and their recording with reference to the current time.

(5) Receiving the external data required for the GTS work and issuing the information on GTS condition to investigators.

To solve these problems, the ground-based equipment was designed and fabricated to work at frequencies corresponding to those on board the HIRC, including the highly sensitive system of receiving the scientific and service data at a frequency of 15 GHz, the transmitter-receiver system to work at 7.2/8.4 GHz, the system for recording and primary processing the scientific and service data, the system of reference frequencies with an H-maser, and the time service with a GPS receiver. The RT-22 antenna was supplied with an especially developed feed system (FS) to work at the quoted frequencies.

The onboard HIRC was subjected to a variety of trials and verifications, including tests carried out jointly with the onboard SRT research complex. The GTS complex was tested according to a specific program of ground drills, as well as jointly with the onboard SRT scientific complex. The ability of the ONBOARD—EARTH link was confirmed to reliably receive scientific and service data.

THE DATA PROCESSING CENTER OF THE SPACE INTERFEROMETER

The results of scientific research carried out at the space interferometer are eventually processed and interpreted at the data processing center of the Astro Space Center of the Lebedev Physics Institute (ASC LPI), as well as at the processing centers of other project members. First, the cross-correlation method is used to process the data flows that are recorded at different radio telescopes, including the space segment of the SRT, using the RDR-1 recording system created at the ASC LPI (the recording density is 256 Kb/s).

A software FX correlator of the ASC is based on an effective computing cluster with a performance of 1 TFLOP/s and the RAID data storage system with a capacity of up to 220 TB (Fig. 3).

The cross-correlation function of signals from separate interferometers is calculated using the computer realization that includes the following operations:

Fourier transform—multiplication—inverse Fourier transform.

In contrast to current hardware correlators, this sequence of operations enables us to enhance appreciably the performance of data processing, to control



Fig. 1. Onboard high-information radio complex.

functionality and multimode properties of this process without additional financial expenses.

The software correlator of the ASC LPI accepts data in any VLBI format currently utilized. To synchronize the data flows within one μ s, the mission uses precision analytic models of the *Radioastron* SC motion and actual distant ballistic measurements of its orbital parameters provided by the interpretation center of trajectory measurements of the Institute of Applied Mathematics (Russian Academy of Sciences) (Fig. 4).

Table 1. Large ground-based radio telescopes

Telescope	Diameter of the antenna (m)	SRT bands
Arecibo (the United States)	300	P, L, C
GMRT (India)	246	P
VLA (the United States)	125	P, L, C, K
GBT (the United States)	100	P, L, C, K
Effelsberg (Germany)	100	L, C, K
WSRT (the Netherlands)	93	P, L, C
Jodrell Bank (England)	76	P, L, C
DSN Goldstone (the United States)	70	L, K
DSN Robledo (Spain)	70	L, K
DSN Tidbibilla (Australia)	70	L, K
Evpatoriya (Ukraine)	70	P, L, C, K
Ussuriisk (Russia)		P, L, C, K ?
Parkes (Australia)	64	P, L, C, K
Kalyazin (Russia)	64	L, C
Usuda (Japan)	64	L, C, K
Sardinia (Italy)	64	P, L, C, K

Note: Radio telescopes with antenna diameters greater than 60 m that are involved in some observational programs together with the *Radioastron* radio telescope.

Table 2. The strongest and most interesting compact extragalactic sources

IAU name	Other designations	z	S (Jy)	θ_{\max} (ms of arc)	θ_{\min} (ms of arc)	T_b (10^{13} K)	N_o	N
1	2	3	4	5	6	7	8	9
0420-014		0.915	7.62	0.09	<0.02	>5.18	6	4
0528+134		2.07	4.21	0.22	<0.03	>2.06	6	3
0716+714		(0.3)	2.51	0.08	<0.01	>1.85	6	5
1055+018	4C+01.28	0.888	4.28	0.23	<0.02	>1.36	8	5
1334-127		0.539	7.17	0.16	<0.01	>3.19	6	4
1730-130	NRAO530	0.902	7.49	0.23	<0.03	>1.50	7	5
1741-038	OT-068	1.057	4.55	0.16	<0.02	>2.03	3	1
1749+096	4C+09.57	0.320	5.13	0.16	<0.02	>1.34	6	4
2230+114	CTA 102	1.037	3.11	0.12	<0.03	>1.27	9	5
2255-282		0.927	5.50	0.13	<0.02	>2.24	2	1
0642+449	OH471	3.408	1.67	0.21	0.08	0.43	6	4
0851+202	OJ 287	0.306	3.32	0.12	<0.05	>0.39	10	7
1226+023	3C 273	0.158	7.36	0.13	<0.06	>0.17	15	11
1228+126	M87	0.004	0.73	0.41	<0.27	>0.007	13	5
1253-055	3C279	0.538	11.21	0.30	<0.05	>0.88	14	8
1508+572	VSOP	4.309	(0.1)					
1937-101		3.787	0.16	0.30	0.12	0.015	2	0
2200+420	BL Lac	0.069	2.78	0.37	<0.03	>0.15	14	10
2251+158	3C454.3	0.859	3.77	0.26	0.11	0.105	11	4

Columns: 1—IAU name of the source; 2—other designations; 3—redshift; 4, 5, 6, 7—flux, maximum and minimum size, and brightness temperature of an unresolved detail at 15 GHz; 8—number of observational epochs; 9—number of observational epochs when an unresolved detail was observed [3].

The operational rate of the ASC cluster makes it possible to receive the data flows from ten stations (including the *Radioastron* SRT) with a general density of 2.56 Gb/s and, accordingly, to process the flows from 45 interferometers formed in the experiment. This occurs almost without decreasing the input rate of observational data incoming in real time.

Apart from the correlator, there is a graphic user interface ASL that is supported to implement pro-



Fig. 2. Ground tracking station based on RT-22 (Pushchino).

grams for solving specific astrophysical problems associated with the following objects:

- (1) the sources with continuous spectra of radiation;
- (2) the sources of monochromatic maser radiation (molecular lines OH and H₂O);
- (3) the sources of pulse radiation with a continuous spectrum (pulsars); the aim is to determine the parameters of the medium in the Galaxy where the signals propagate.

The cycle of interferometric experiments was carried out in the SRT (ASC LPI) frequency bands jointly with national and foreign radio telescopes in 2010–2011 to verify the hardware and software required for data processing in the *Radioastron* project. The sensitivity of the emulated facility and the quality of the results showed that they fully conformed to all the specifications.

KEY AREAS OF THE SRT SCIENTIFIC RESEARCH

The method of multifrequency synthesis (MFS) imaging is supposed to be implemented for the shortest wavelengths (K-range) in the *Radioastron* project [2]. One channel with circular polarization will operate at a fixed frequency of 22.232 GHz. The second channel (operating simultaneously) with circular polarization of opposite orientation will have the



Fig. 3. Computing cluster with ten servers (performance of 1 TFLOP/s): (a) data storage with capacity of 220 TB; (b) backup device.

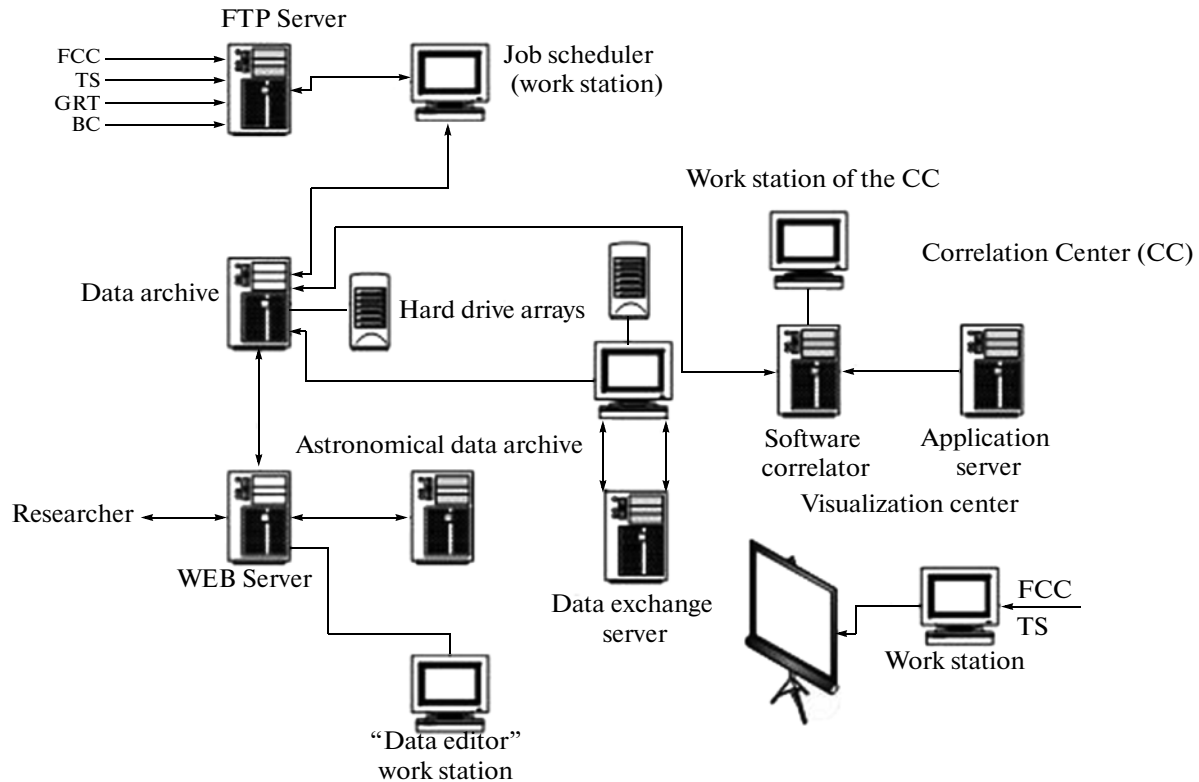


Fig. 4. Scheme of the data processing center at the Astro Space Center of the Lebedev Physics Institute.

capability to switch in the range 18.392–25.112 GHz, i.e., $f_{\max}/f_{\min} = 1.37$. This will make it possible to obtain one-dimensional images over the time that is determined by the integration time of each channel multiplied by the number of switched frequencies. Two-dimensional images can be obtained twice per orbit with the maximum angular resolution, where the filling of an elliptical region in the spatial UV frequency plane is $1 - (f_{\min}/f_{\max})^2 = 46\%$. It is important to note that this value does not depend on the dis-

tances and other orbital parameters. In general, the channel with the fixed frequency is fully compatible with the ground-based radio telescopes. The frequency-tuned channel will be compatible with the same band of the K range of especially prepared ground-based radio telescopes.

Some advantages of the MFS method are as follows:

(1) It is possible to obtain one-dimensional images of sources with the highest angular resolution in less than an hour for any part of the orbit;

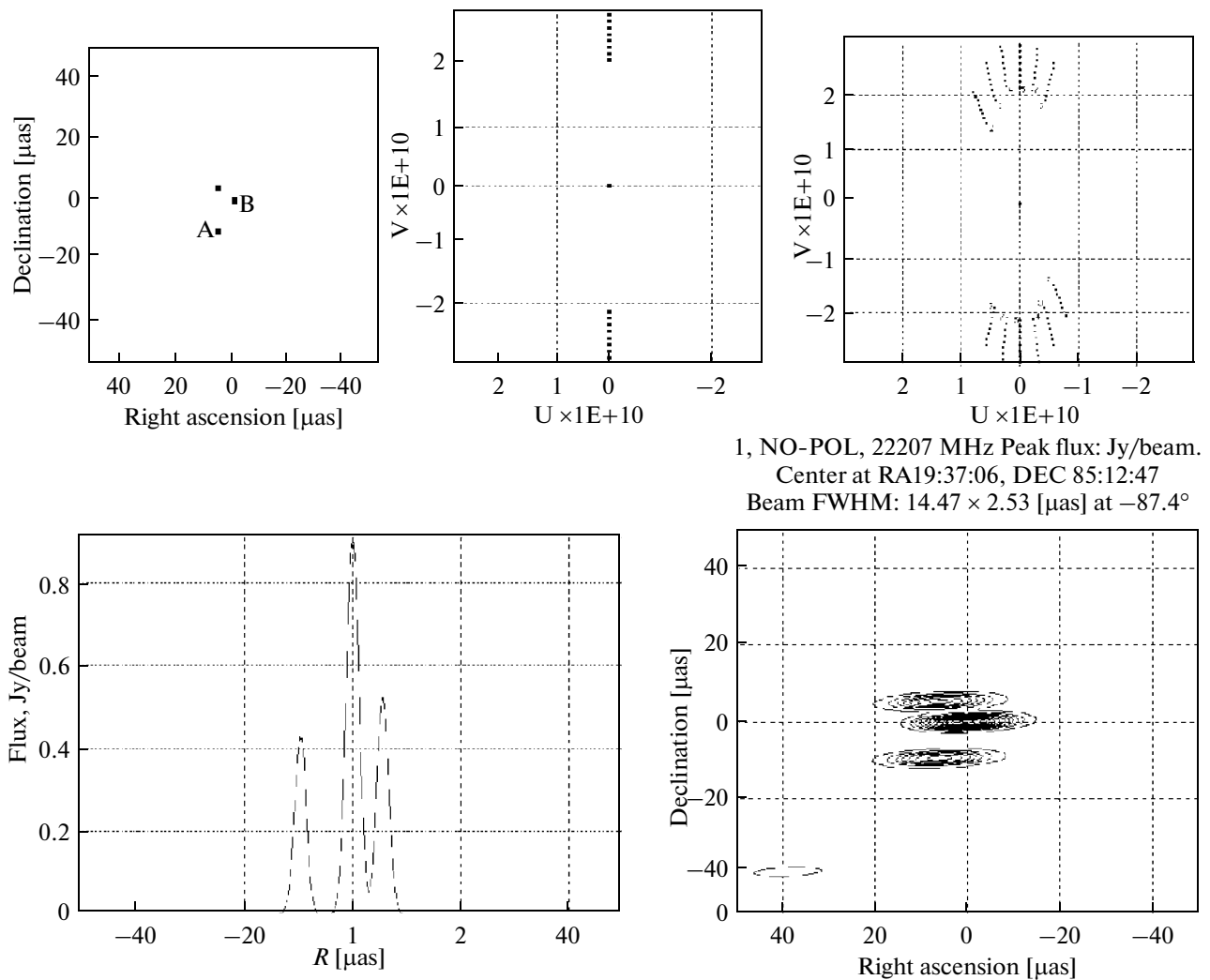


Fig. 5. Simulation of the MFS method applied in Radioastron project [2].

Top left: true image (three point-like sources with the fluxes $F_A = 0.5$, $F_B = 1.0$, and $F_C = 0.5$, in arbitrary units; $AB = 12 \mu$ s, $AC = 15 \mu$ s, and $BC = 9 \mu$ s). Top center: coverage of the UV plane when switching among eight frequencies of the K channel; bottom left: one-dimensional image obtained as a result of this switching. Top right: coverage of the UV plane after five switchings among frequencies as the telescope passes a 5-day path in orbit; bottom right: the corresponding two-dimensional image.

(2) Two-dimensional images can be obtained during 3–5 days in any part of the orbit or during 0.5–1 day near perigee;

(3) It is possible to obtain spectra in the K range for different image details;

(4) The angular size of an image can be determined as a function of frequency associated with the scatter, absorption, or other physical processes;

(5) Maps of linear polarization and Faraday rotation measures, or a map of circular polarization, can be produced and the degree of polarization can be determined as a function of frequency;

(6) Differential coordinates and proper motions can be determined with a very high accuracy;

(7) Physical variability of the source structure and/or variability due to interstellar plasma or plasma

in the envelope of the source can be studied as a function of frequency.

To realize these goals, a corresponding observational mode can be chosen that is determined by the central frequency of the tuned channel, namely, 18.392, 19.352, 20.312, 21.272, 22.232, 23.192, 24.152, and 25.112 GHz. The bandwidth for each frequency is 32 MHz.

Figure 5 shows the results of numerical simulation for a one-dimensional and two-dimensional map of the source consisting of three point-like components [5].

One of the main tasks of the scientific research program of the *Radioastron* space interferometer will be studying the structure and dynamics of central regions of extragalactic radio sources of synchrotron emission, which will possibly enable us to obtain information from regions near the event horizons of supermassive

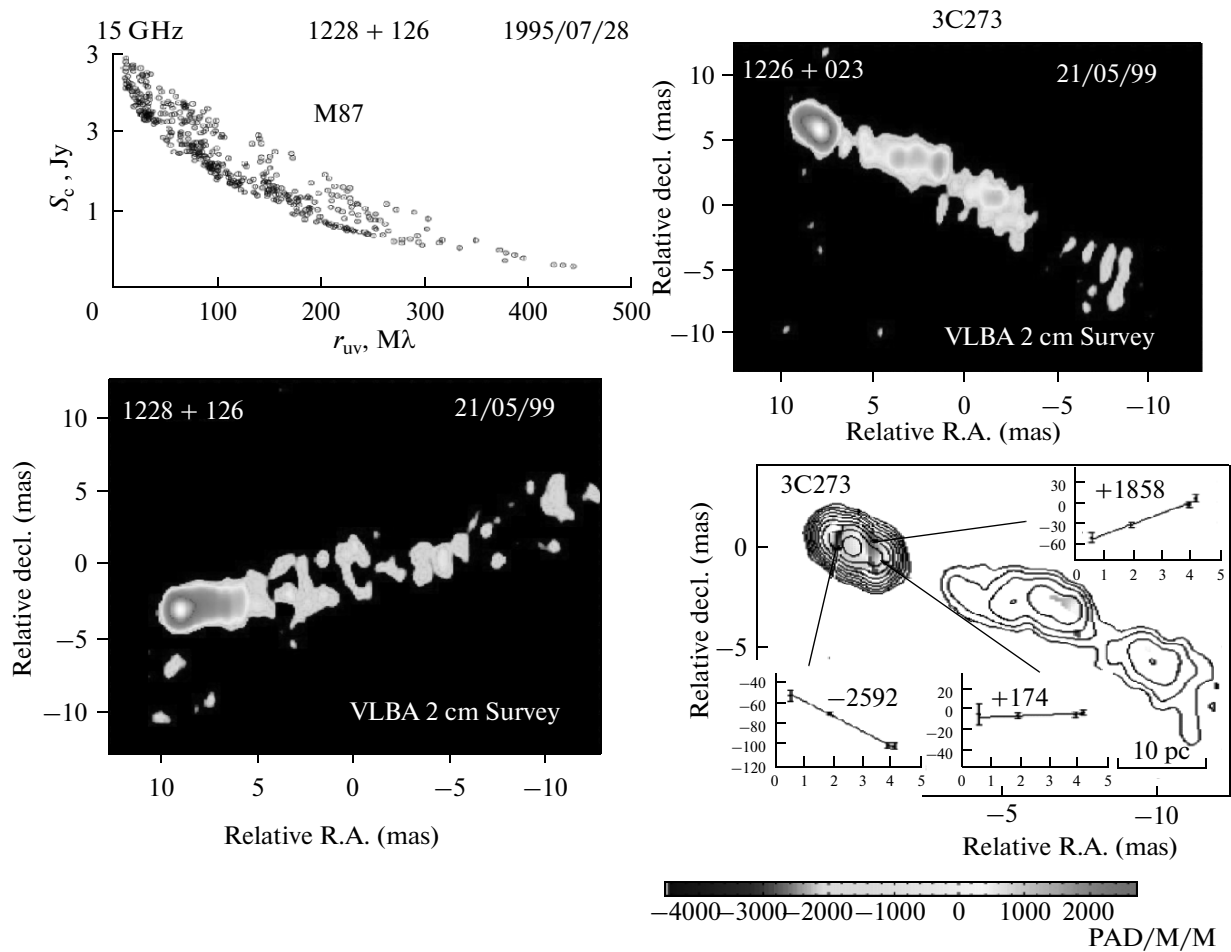


Fig. 6. Radio galaxy M87 and quasar 3C273 are the most important extragalactic objects for study in the Radioastron project. Top left: correlated flux density of M87 as a function of baseline projection of the ground-based VLBA interferometer at 15 GHz; bottom left: the corresponding image. Top right: image of 3C273 at the same instrument; bottom right: polarization angle as a function of observation frequency.

black holes. Extensive studies of the structure and spectra of extragalactic objects, as well as the detection of components unresolved on Earth, were carried out using many ground-based radio telescopes and the VLBA global interferometer at 15 GHz [3]. The strongest and most interesting compact sources are gathered in Table 1.

Figure 6 (left) shows the image of radio galaxy Virgo A (M87) and the observed flux of the radio emission as a function of interferometer baseline, i.e., the angular resolution in observations at a wavelength of 2 cm using the VLBA antenna.

The center of M87 contains a supermassive black hole that is one of the largest currently known. Its mass is 6.6 billion solar masses [4]. Figure 6 shows that the central part of the object cannot be resolved even for the largest baselines. It will be possible to study the structure of the innermost parts of this object using the *Radioastron* interferometer for the first time; maybe, we will be even able to look inside (if it is an entrance to a wormhole rather than a black hole). The mini-

um fringe width of the *Radioastron* interferometer is seven arc microseconds; it will be possible to measure the size of a source to within a part of the fringe (depending on the signal-to-noise ratio), e.g., one-tenth of the fringe; this implies that the expected angular resolution will be better than one arc microsecond. The expected size of the black hole silhouette, i.e., the diameter of the Schwarzschild sphere around the black hole will be $2R_s = 4GM/c^2 = 14.6 \mu\text{s}$. The expected diameter of a circular orbit for light near a nonrotating black hole ($a = 0$) $(108)^{0.5}GM/c^2 = 37.8 \mu\text{s}$. The diameter of the silhouette of an extremal rotating black hole ($a = 1$) is $9GM/c^2 = 32.8 \mu\text{s}$ and the shift of the image center is $(5)^{0.5}GM/c^2 = 8.1 \mu\text{s}$ [4].

Figure 6 (right) shows also the image of the quasar 3C273 at a wavelength of 2 cm [3] and the variations of polarization plane as a function of observational frequency [5]. This object has one of the strongest radio emission fluxes among radio sources. It is especially interesting because it seems to have a one-sided jet of relativistic particles. One possibility for explaining this

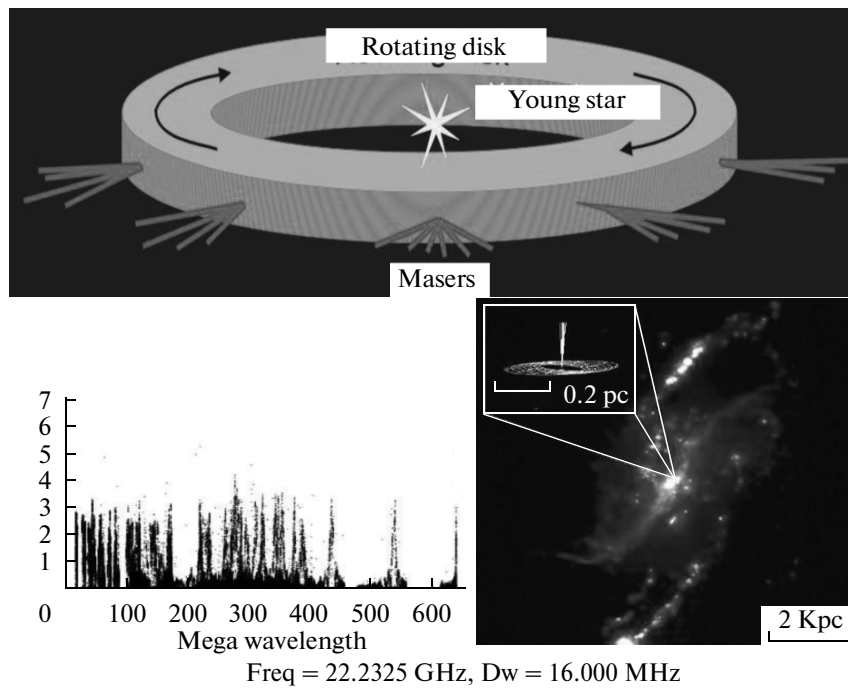


Fig. 7. Model for generating the radio lines.

Top: model of star formation region with masers; bottom left: observed VLA correlated H₂O maser flux (22 MHz) for the region W3(OH) as a function of the interferometer baseline (millions of wavelengths are plotted along the horizontal axis) [10]. Bottom right: H₂O megamaser and H α line image of galaxy NGC 4258 (distance of 6.4 Mpc) [11].

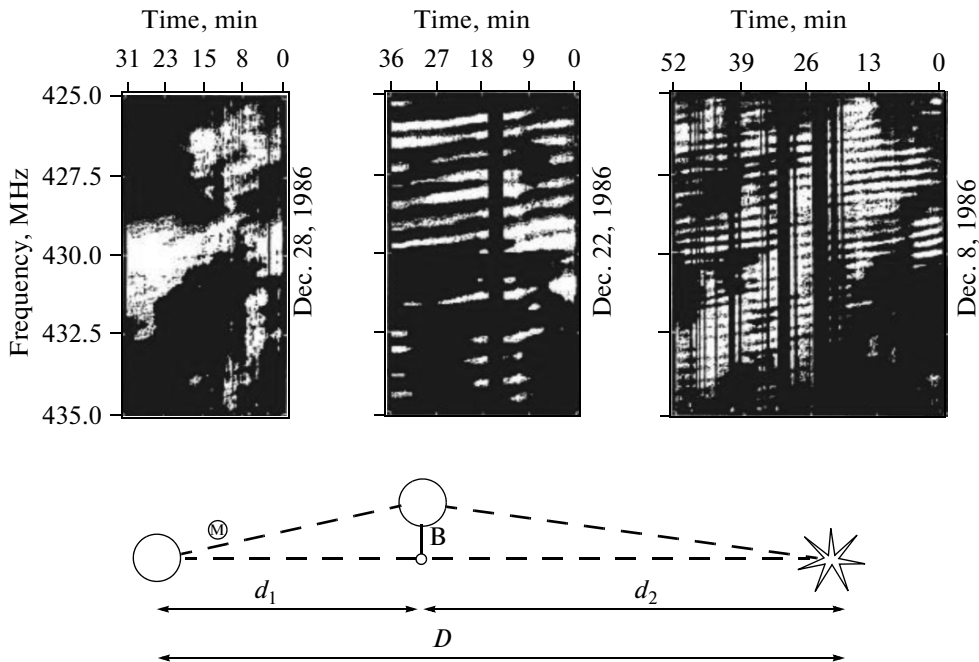


Fig. 8. Dynamic spectrum of oscillation observed for the pulsar PSR 1237+25 with the Arecibo telescope at 430 MHz [12].

Top: dynamic spectrum of the pulsar PSR 1237+25 (period 1.4 s; distance 560 pc). Bottom: scheme of a two-beam “interstellar” interferometer.

structure is to assume that it is an entrance to a worm-hole rather than a supermassive black hole [6].

The most essential question to answer when measuring the polarization of both objects is whether the

magnetic field around the central object has a dipole- or monopole-like structure. Perhaps the structure of the magnetic field is more complicated. The dipole character is anticipated if the magnetic field is due to

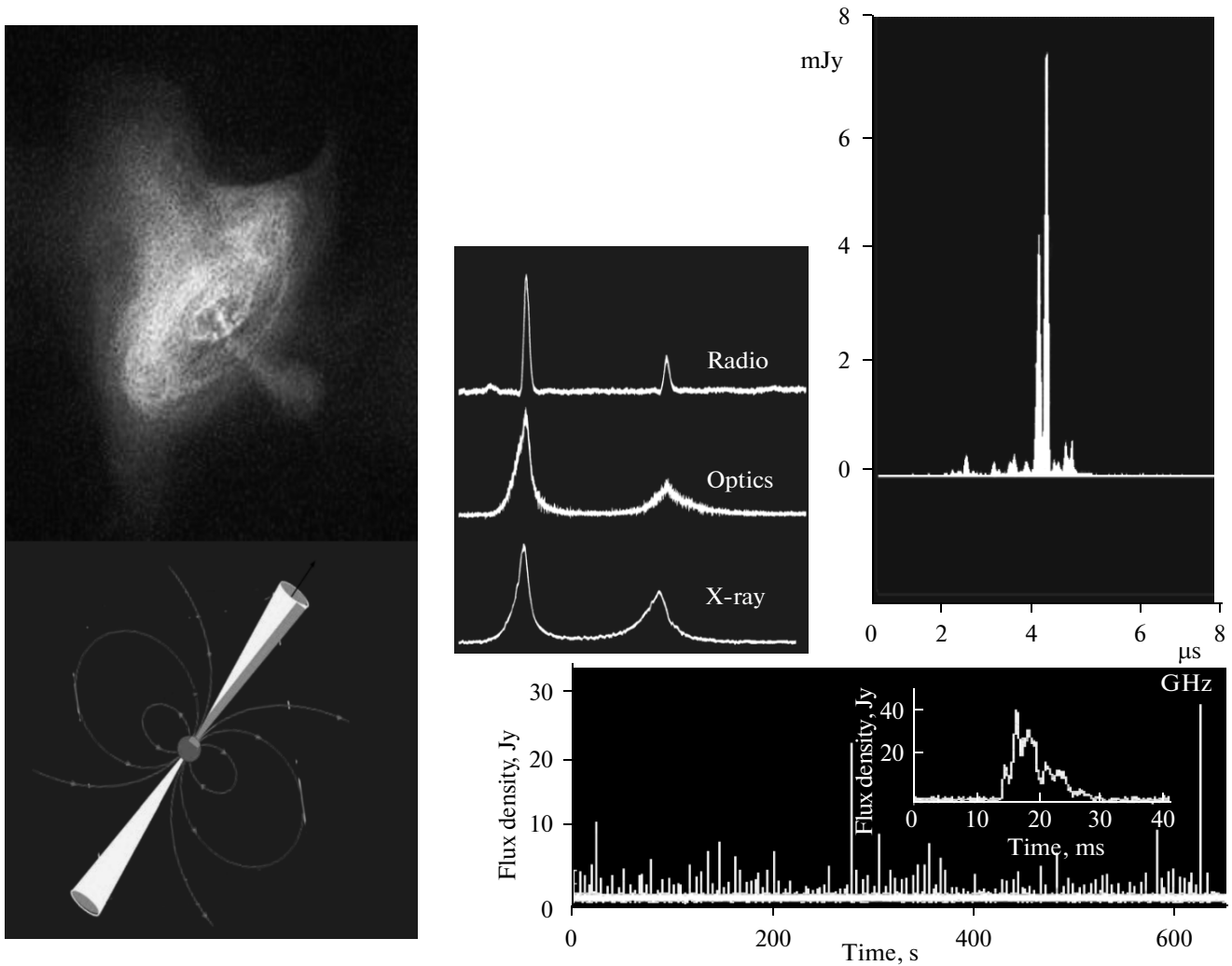


Fig. 9. Observations of XTE J1810-540.

Top right: super giant radio pulse from the Crab pulsar detected with RT-64 at Kalyazin (near-Earth flux is 7 MJy at 2.2 GHz, brightness temperature $T > 10^{40}$ K, electromagnetic field $H > 10^{12}$ Gs) [15]. Top left: X-ray image of the Crab pulsar obtained with the Chandra observatory. Bottom left: model of a rotating neutron star with magnetic field. Center: ordinary pulses from the neutron star in radio, optics, and X-ray range over the course of 33 ms (rotation period of the neutron star). Bottom right: emission from the source XTE J1810-540 observed with the GBT telescope at 42 GHz (sometimes it is a radio emitting magnetar, period 5.54 s, magnetic field 2.6×10^{14} Gs) [14].

the accretion disk rotating around a supermassive black hole. The measurements of Faraday rotation near the core of 3C273 suggest that the opposite sides have opposite signs of rotation relative to the central object and, hence, opposite signs of magnetic field. This could be observational evidence for a monopole structure of the magnetic field. If this is the case, it may indicate the existence of an entrance to a wormhole or a black hole with a magnetic charge (former wormhole).

Another important research direction is to discover where the cosmic ray sources are located in the Universe. Data obtained at the Pierre Auger observatory indicate that cosmic particles with the highest energies observed near the Earth come from the nearest radio galaxy Centaurus A (NGC 5128), from a distance of 3.5 Mpc. The mass of the black hole inside Cen A is 5.5×10^7 solar masses, i.e., approximately one-hun-

dredth that of M87. This implies that extragalactic sources of powerful synchrotron radiation generate, at the same time, cosmic rays of the highest energies; if so, relativistic protons in the sources can also produce synchrotron radiation that we can try to detect.

The ratio of the limiting brightness temperatures for relativistic protons and electrons (if the intensity is bounded by the Compton scattering of the same radiation) is $T_p/T_e = (m_p/m_e)^{6/5} = (1830)^{6/5} = 8821$, where m_p and m_e are the rest masses of the proton and electron, respectively. If the limiting temperature of the synchrotron radiation of relativistic electrons is $T_e = 10^{12}$ K, then the expected limiting radiation temperature of relativistic protons is $T_p = 8 \times 10^{15}$ K. For the given radiation flux, $F_\nu \propto (T/\lambda^2)\Omega \propto T/B^2$, where T is

Earth's gravitational field and GTR

Measurement of anomalous accelerations to within 10^{-10} m/s^2 and construction of the Earth's gravitational potential at large distances;

Testing GTR effects (transverse Doppler effect, clock rate, improving the measured values of frequency redshift by two orders of magnitude, verifying the $1/R^2$ law of the gravitational interaction of bodies).

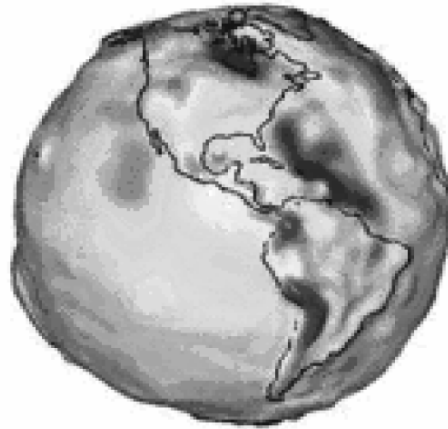


Fig. 10. Research topics to study the Earth's gravitational field using the data of interferometric observations and high-accuracy measurements of the the Radioastron orbit and its evolution.

the brightness temperature, Ω is the solid angle of the source, B_e and B_p are the projections of the interferometer baseline on the plane of the sky (for the source emitting electrons or protons) that are required to resolve the source with the given flux for the limiting brightness temperatures. Then, $B_p/B_e = (m_p/m_e)^{3/5} = 90$. Therefore, interferometers with appreciably larger baselines are required to resolve the sources of synchrotron radiation of protons compared to electrons.

The synchrotron radiation of relativistic protons can be detected by very high brightness temperatures that exceed the limit for relativistic electrons. It is important to have in mind, however, that the brightness temperature can increase due to the motion of the source toward the observer (Doppler enhancement), which can be controlled using the angular velocity measurements of proper motion or expansion of the source. Only the use of high angular resolution will make it possible to establish whether or not a stable source with a temperature of, say, 10^{15} K is observed. This would suggest that a generator of cosmic rays is really observed and provides the opportunity for us to study all its parameters.

Many extragalactic sources show strong variability in observed radio emission flux. Such evidence enables us to give a lower bound for the brightness temperature. Thus, the variability of the source 0716+714 on timescales of less than one day implies that its brightness temperature is greater than 10^{15} K and even 10^{19} K [9]. Such a brightness temperature must correspond to a Lorentz factor of 90 in the Doppler enhancement model and this can only be verified using the space interferometer.

The above sections of the research program were associated with the study of sources of synchrotron radiation that covers many frequency bands. The objects with narrow-band maser radiation are another kind of strong source, which are qualitatively different.

Powerful narrow-band radiation is observed in the lines of some molecules associated with the regions of young stars and planetary system formation. Figure 7 shows a model for generating this radiation in a star formation region and the observational results obtained for a water vapor line in the source W3(OH) at 22 GHz using the VLBA interferometer [10]. The baseline is measured along a horizontal axis and the correlated flux is plotted on the vertical axis. It can be seen that the source is very compact and cannot be resolved even with the largest baselines. Figure 7 shows also the sources of maser radiation in the same spectral line near the nucleus of the galaxy NGC 4258 [11]. Compact regions that emit in the water vapor line are observed around the central object (possibly a black hole). The regions are shown by dots; red and blue dots denote motions away from and toward us, respectively. This class of observed objects is referred to as megamasers; they are not yet resolved in detail and will be studied in the future. The expected limiting brightness temperatures for them may be up to 10^{16} K [10]. Together with the structure of star-forming complexes and sizes of individual regions, parallaxes and proper motions of maser sources can be determined using the space interferometer, which is a very important research direction for constructing a model of our galaxy and other galaxies and for improving cosmological theory.

A coherent radiation mechanism can ensure higher brightness temperatures as well. This mechanism is likely to be responsible for the radio emission of pulsars (neutron stars). However, the sizes of these objects (even nearest of them) are too small to be resolved even with the space interferometer. Figure 8 illustrates the method that, as a matter of fact, has not yet been used in radio astronomy. It can be only realized using special observations with the space interferometer. This method proposes observation of scintillations of the correlated signal due to inhomogeneities of the interstellar plasma. Scintillation appears as a result of

the superposition of the signals that passed through the medium along different paths. This implies that interferometers with far greater baselines appear naturally as beams pass through the clouds of interstellar plasma. Figure 8 shows the dynamic spectrum of scintillation observed for the pulsar PSR1237+25 with the Arecibo telescope at 430 MHz [12]. Time is plotted on the horizontal axis and frequency on the vertical axis. A clear striped pattern corresponds to that expected for two-beam signal propagation, i.e., for a two-antenna interferometer with a very large space baseline; however, there are no data available so far on the appearance of this pattern in different regions of space near the Earth. Such a distinct interference that corresponds to two-beam signal propagation is observed rarely. Generally, a more complicated dynamic spectrum can be seen and multi-beam signal propagation takes place, but the parameters of the effective interstellar interferometer can be determined in those cases as well [13]. This method, combined with the *Radioastron*, will possibly give resolutions hundreds or thousands of times greater than those using the Earth-space interferometer.

Lately, a new class of pulsars was discovered referred to as magnetars (PSR J1550-5418 with a period of 2.069 s and XTE J1810-5408 with a period of 5.54 s). Magnetars have anomalous flat spectra or even increasing for higher frequencies in the cm and mm bands [14]. It is extremely interesting how coherent radiation can arise at such high frequencies (that is, how tiny charge inhomogeneities can form). At the same time, these objects are transient X-ray sources. Their pulsed radio emission appears sporadically too. Figure 9 (bottom right) shows observational data obtained for XTE J1810-540.

For some pulsars, individual pulses were detected with amplitudes that exceeded the mean value by many orders of magnitude. In particular, such pulses are observed from the Crab pulsar with a periodicity of approximately one pulse per hour. These pulses have brightness temperatures of 10^{40} K, which is an absolute record [15]. This is a very interesting research topic, to study phenomena in the magnetospheres of neutron stars responsible for gigantic pulses; moreover, observation of these pulses can be of great importance in practice because it can be used to synchronize time all over the Earth provided that the pulse is observed at many sites and on board the *Radioastron* (Fig. 10).

Figure 10 shows also the map of gravitational anomalies constructed using the observations on board the low-orbit *GRACE* satellite [16]. The *Radioastron* will be able to produce the gravitational field pattern up to very large distances.

The *Radioastron* space observatory is scheduled for launch in the current year. The scientific research program, in accordance with technological capabilities and spacecraft mission life time, is expected to last at least five years.

REFERENCES

1. www.asc.rssi.ru/radioastron/index.html
2. Andreyanov, V.V., et al., Multi-Frequency Reception Method for Radio Images Synthesis in the *Radioastron* Project, in *Radioastronomical Tools and Techniques*, Kardashev, N.S. and Dagkesamanski, R.D., Eds., Cambridge Sci. Publ., 2007, pp. 17–26.
3. Kovalev, Y.Y., Kellermann, K.I., Lister, M.L., Homan, D.C., Vermeulen, R.C., Cohen, V.H., Ros, E., Kadler, M., Lobanov, A.P., Zensus, J.A., Kardashev, N.S., Gurvits, L.I., Aller, M.F., and Aller, H.D., *Astron. J.*, 2005, vol. 130, p. 2473; Kellermann, K.I., Lister, M.L., Homan, D.C., Vermeulen, R.C., Cohen, M.H., Ros, E., Kadler, M., Zensus, J.A., and Kovalev, Y.Y., *Astrophys. J.*, 2004, vol. 609, p. 539; Vol'vach, A.E., Vol'vach, L.N., Kardashev, N.S., and Larionov, M.G., *Astron. Rep.*, 2008, vol. 52, p. 429; Mingaliyev, M.G., Sotnikova, Yu.V., Bursov, N.N., Kardashev, N.S., and Larionov, M.G., Spectral Characteristics of Radio Sources near the North Celestial Pole, *Astron. Rep.*, 2007, vol. 51, issue 5, pp. 343–363.
4. Gebhardt, K.A., Jr., Richstone, D., Lauer, T., Gultiken, K., Murphy, J., Faber, S., and Tremaine, S., arXiv: 1101.1954; Broderick, A.T. and Loeb, F., *Astrophys. J.*, 2009, vol. 697, pp. 1164–1179.
5. Zavala, R.T. and Taylor, G.B., Time-Variation Faraday Rotation Measures of 3C 273 and 3C 279, *Astrophys. J.*, 2001, vol. 550, p. L147.
6. Kardashev, N.S., Novikov, I.D., and Shatskii, A.A., Magnetic Tunnels (Wormholes) in Astrophysics, *Astron. Rep.*, 2006, vol. 50, no. 8, p. 601.
7. Bluemer, J., For the Pierre Auger Collaboration, arXiv:0807.4871.
8. Kardashev, N.S., Synchrotron Radio-Frequency Radiation Caused by Protons and Electrons in Pulsars and Quasars, *Astron. J.*, 2000, vol. 77, p. 813.
9. Fuhrmann, L., et al., Testing the Inverse-Compton Catastrophe Scenario in the Intra-Day Variable Blazar S5 0716+71. III. Rapid and Correlated Flux Density Variability from Radio to sub-mm Bands, *Astron. Astrophys.*, 2008, vol. 490, no. 3.
10. Slysh, V.I., Self-Stark Limit on Brightness Temperature in Cosmic Masers, *ASP Conf. Proc.*, 2003, vol. 300, p. 239.
11. Miyoshi, M., Moran, J., Herrnstein, J., Greenhill, L., Nakai, N., Diamond, P., and Inoue, M., Evidence for a Black Hole from High Rotation Velocities in a sub-Parsec Region of NGC 4258, *Nature*, 1995, vol. 373, p. 127.
12. Wolszczan, A. and Cordes, J.M., Interstellar Interferometry of the Pulsar PSR 1237+25, *Astrophys. J.*, 1987, vol. 320, p. L35; Shishov, V.I., Turbulent Interstellar Plasma and Ultrahigh Angular Resolution in Radio Astronomy, *Astron. Rep.*, 2001, vol. 45, p. 195.
13. Shishov, V.I., Interstellar Scintillation and Nanosecond Resolution in Radioastronomy, *Astron. Zh.*, 2010, vol. 87, pp. 1–4.
14. Camilo, F., Ransom, S.M., Halpern, J.P., Reynolds, J., Helfand, D.J., Zimmerman, N., and Sarkissian, J., Transient Pulsed Radio Emission from a Magnetar, *Nature*, 2006, vol. 442, p. 892.
15. Popov, M.V., Soglasnov, V.A., Kondratiev, V.I., Bilous, A.V., Moshkina, O., Oreshko, V.V., Ilyasov, Yu.P., Sekido, M., and Kondo, T., Multifrequency Study of Giant Radio Pulses from the Crab Pulsar with the K5 VLBI Recording Terminal, arXiv: 0903.2652; Soglasnov, V., Amazing Properties of Giant Pulsars and the Nature of Pulsar's Radio Emission, arXiv: astro-ph/0701190.
16. <http://nasascience.nasa.gov/missions/grace/>